CHEMISTRY OF MATERIALS

pubs.acs.org/cm

Article

Side Chain Effects on the Conductivity of Phenothiazine-Derived Polyaniline

Published as part of Chemistry of Materials virtual special issue "In Honor of Prof. Elsa Reichmanis."

Hari Giri, Guorong Ma, Mohammed Almtiri, Xiaodan Gu, and Colleen N. Scott*

Cite This: *Chem. Mater.* 2024, 36, 2279−2288

Read Online

ACCESS | Metrics & More | Article Recommendations | Supporting Information

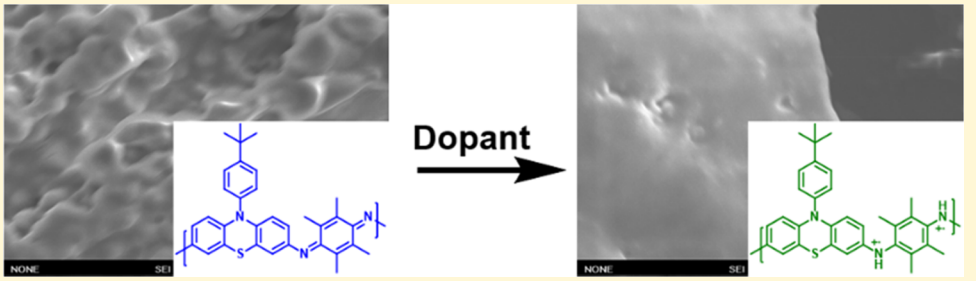

ABSTRACT: Side chain alkyl groups have become the standard for incorporating solubilizing groups into conjugated polymers. However, the variety of alkyl groups available and their location on the polymer's backbone can contribute to the packing of the polymer chains in many different ways, resulting in many different morphologies in the polymer that can affect its properties and performances. In this paper, we investigate the effects on the conductivity of nine phenothiazine-containing polyaniline derivatives (**P1**−**P9**) with alkyl or aryl side chains on the phenothiazine core while also varying the number of methyl groups on the *p*-phenylenediamine unit. ^{1}H nuclear magnetic resonance spectroscopy, ultraviolet−visible spectroscopy, differential scanning calorimetry, scanning electron microscopy, atomic force microscopy, and wide-angle X-ray scattering (WAXS) were all used to study the polymers' structures, physical and thermal properties, and morphologies. The *t*-butylphenyl substituent on the phenothiazine core seems to provide more rigidity in the polymer's backbone resulting in higher T_g for series 3, while series 2 containing the 2-hexyldecyl-substituted polymers had the lowest T_g, which is attributed to the large volume of the side chain, that limits interchain interactions. Consequently, series 2 had the lowest conductivity. However, the strongest effect on the conductivity was seen from the tetramethyl groups on the PPDA unit, which resulted in the lowest conductivity in each series due to torsional strain (twisting) in the polymer's backbone. The WAXS data suggest mostly amorphous films; thus, the conductivity in these materials seems to be dominated by a multiscale charge transport phenomenon that occurs in amorphous conjugated materials. Our results will aid in the understanding of side chain engineering of PANI derivatives for their optimum performances.

INTRODUCTION

The discovery of conductive polyacetylene more than 50 years ago was a paradigm shift in the field of polymer science.[1] It has become the driving force today in the field of organic electronics for the development of flexible and affordable electronic devices.[2−5] Conducting polymers (CP) have many attributes that make them unique in comparison to metallic conductors, such as lightweight, transparency, flexibility, low thermal conductivity, ambient temperature processing, synthetic tunability, low-cost production, and solution-based processing.[2,6] Additionally, the prospect of solution and melt processable polymers offers a convenient method for the application of CP coatings and the fabrication of devices on a large scale.[7] Since then, many conducting polymers with simple structures such as polypyrrole (PPy), polythiophene (PTH), poly(paraphenylene) (PPP), poly(phenylenevinylene) (PPV), polyfuran (PF), and polyaniline (PANI) have been prepared. Among them, PANI stands out as the most viable due to its high conductivity, high stability in the doped state, and low-cost production.[6,8,9] Consequently, PANI has been studied for many applications such as corrosion,[10,11] printed circuit boards,[12] antistatic coatings,[13] electrochromic displays,[14] charge storage devices,[15,16] hole transport layers (HTLs) in perovskite solar cells,[17−19] light-emitting diodes (LED),[20] waste removal,[21,22] and biosensors.[23] However, PANI's limited solubility in common organic solvents and its electrochemical instability have prompted our group and others to explore

Received: September 18, 2023
Revised: February 11, 2024
Accepted: February 12, 2024
Published: February 27, 2024

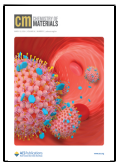

PANI derivatives as alternatives to address PANI's limitations.[24−27] For example, poly(1-naphthylamine) has been studied by Ahmad and co-workers, and later by Riaz's group, in a number of applications such as anticorrosion and antibacterial coatings,[28−30] photolytic degradation of dyes,[31,32] and wastewater remediation.[33] Other aryl- and N-substituted PANI derivatives were also reported to enhance the solubility and were used in various applications. In this regard, Ma et al. reported the synthesis of poly(2,3-dimethylaniline) with improved anticorrosion and electrochemical properties compared to PANI.[34,35] The synthesis of poly(*o*-ethoxyaniline) was reported by Sathyanarayana et al.,[36] while Savitha et al. reported a copolymer, poly(*o*-/*m*-toluidine-*co*-*o*-nitroaniline),[37] that both displayed excellent solubility and anticorrosion properties. Chen and co-workers performed a study on N-substituted PANI with a series of alkyl chains ranging from butyl (C4) to hexadecyl (C16) and showed that their solubilities increased as the size of the alkyl chain increased due to a lowering of the polarity and stiffness of the polymer chains by the flexible alkyl substituent.[38]

Fused ring cores have also been incorporated into the PANI backbone to improve its properties. Phenothiazine, containing three fused rings, is an ideal core to prepare PANI derivatives because of its low cost, accessibility, and strong electron-donating character. Furthermore, its nonplanar "butterfly-type" conformation prevents it from aggregating and forming insoluble polymeric material.[39] While its nonaggregation tendency is attractive for certain applications such as LED, it is less attractive for applications where aggregates are necessary. When it is incorporated into the backbone of conjugated polymers, the lack of planarity in the phenothiazine core may affect the packing of polymer chains. Additionally, the incorporation of side chains onto the backbone, aimed at enhancing solubility/processability, could significantly modulate the nature of the phenothiazine core and thus the polymer.[40] Our group has recently published three PANI derivatives containing fused heterocyclic rings (phenoxazine,[41] carbazole,[42] and phenothiazine[43]) functionalized with branch chain alkyl groups and copolymerized with *p*-phenylenediamine (PPDA). They were used as charge storage devices[42] and as second HTL in perovskite solar cells (PSCs)[43] due to their high solubility and excellent electrochemical stability. Liu et al. also prepared copolymers with phenothiazine and phenazine for organic cathode battery material.[44] In these reports, there is no mention of the effect of the phenothiazine ring or the side chain substituents on the properties of the polymers.

Research efforts are ongoing to explore the effects of the side chains on the optoelectrical properties of conjugated polymers.[45−47] These studies have garnered increasing interest in various fields due to the potential to enhance the mechanical properties and processability of the polymers. The size of the side chains influences the temperature for thermal transition, solubility, mechanical property, and packing/ordering of conjugated polymers, which ultimately affects their conductivity.[40,48] However, the investigation of novel side chains remains a relatively infrequent area of research.[49] In the case of conventional alkyl side chains, it is commonly observed that the presence of branched alkyl chains tends to enhance solubility and enhance the performance of devices in conjugated polymers, in comparison to linear alkyl chains.[40] However, there is always competition between the insulating alkyl side chains and the packing of the conjugated backbone.[49,50] For PANI, the flexibility of the films was observed when the side chain is relatively long and/or branched.[51] In particular, the presence of side chains impacts various aspects of the polymer such as the doping mechanism and efficiency, long-range ordering and polymer packing, and the morphology of blends that consist of polymers and discrete molecules.[52−54]

In this paper, we report our results from the investigation of side chain effects on the conductivity of phenothiazine-containing PANI derivatives. Interesting microstructures may arise when the amine nitrogen of phenothiazine is functionalized, or other bulky structures are present in the polymer's backbone. It has been shown that small changes in the alkyl side chains can have large effects on the polymers' morphology.[55,56] For these reasons, we explore the effects of N substituents on the phenothiazine core and methyl substituents on the bridging PPDA group on the packing and subsequent electrical conductivity of some PANI derivatives. Nine polymers are prepared with three different substituents on the phenothiazine nitrogen, and each phenothiazine unit is copolymerized with three different PPDA groups. The structure of the polymers (**P1−P9**) is characterized by proton nuclear magnetic resonance (^{1}H NMR) and Fourier-transform infrared spectroscopy (FTIR), while size exclusion chromatography (SEC) is used to determine their molecular weights (M_n). Absorption (ultraviolet−visible, UV−vis) spectroscopy is used to analyze their doped and undoped states. Furthermore, the polymers' conductivity is determined by a four-point probe, while scanning electron microscopy (SEM), atomic force microscopy (AFM), and wide-angle X-ray scattering (WAXS) techniques are used to analyze the polymers' morphology.

EXPERIMENTAL SECTION

Unless otherwise stated, all reagents were purchased from commercial suppliers and used as is without additional purification. All compounds were of reagent grade. The solvents (THF, DMF, DCM, and toluene) were all distilled overdrying agents. Oven-dried glassware was used for the reactions. Air or moisture-sensitive reactions were executed under an inert atmosphere of nitrogen. ^{1}H NMR spectra were recorded at 500 MHz at room temperature on a Bruker spectrometer with the deuterated solvent. The chemical shifts were expressed in parts per million downfield from $SiMe_4$. The NMR data were processed by Mestre Nova. $CDCl_3$ was employed as the solvent unless otherwise stated, with the reference peak at 7.26 ppm. The coupling constants (J) were stated in Hz. Multiplicities were denoted by the letters s (singlet), d (doublet), t (triplet), q (quartet), and m (multiplet). The product was purified by performing Flash chromatography on Combi Flash Rf+ Purlon with silica gel (300−400 mesh) containing 60 pore size. Flash columns were commercially packaged and purchased from Silicycle. Thin-layer chromatography (TLC) was carried out on 50 mm × 20 mm aluminum-backed silica gel and observed with a UV lamp at 254 nm. The determination of number-average molecular weight (M_n), weight-average molecular weight (M_w), and polydispersity index (PDI) was conducted using TOSOH EcoSEC gel permeation chromatography (GPC) calibrated by monodisperse polystyrene standards. The ultraviolet−visible (UV−vis) spectra of polyaniline derivatives and PANI were collected in a 1 cm quartz cell using an Agilent (Cary 60) spectrophotometer. The spectrum was recorded between 200 and 1100 nm. Thermogravimetric analysis (TGA) measurements were carried out on TA Q50 equipment. Experiments were conducted in a nitrogen stream with a flow rate of 50 mL per minute and a scanning rate of 10 °C per minute throughout a temperature range of 30−1000 °C. Measurements using differential scanning calorimetry (DSC) were carried out with a Q2000 calorimeter (TA Instruments, USA) in a

https://doi.org/10.1021/acs.chemmater.3c02268
Chem. Mater. 2024, 36, 2279−2288

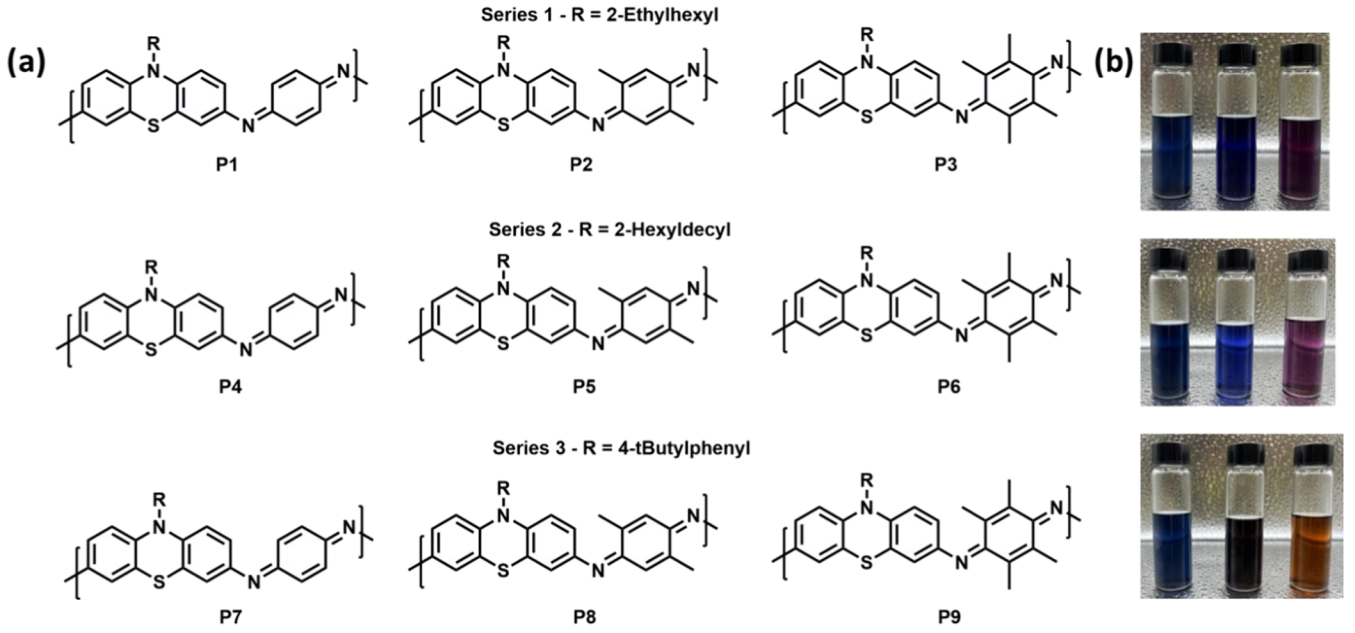

Figure 1. Structures of the polymers (a) and color of each polymer in DCM (b).

stream of nitrogen at a scanning rate of 10 °C per minute using aluminum pans. The samples were subjected to a heat/cool/heat cycle, with the cooling and second heating cycles reported below. Samples were heated and cooled at a rate of 10 °C/min over a window chosen based on TGA degradation temperatures. Samples were tested at temperatures between 0 and 250 °C in aluminum pans. The infrared spectra (ATR−FTIR) of powder polymers were acquired between 4000 and 400 cm^{-1} in a Cary 630 instrument provided with diamond attenuated total reflectance (ATR). Data are reported in wavenumbers (cm^{-1}). WAXS of powder was performed on a laboratory beamline system (Xenocs Inc. Xeuss 2.0) with an X-ray wavelength of 1.54 Å and a sample−detector distance of 13 cm. Samples were kept between the Kapton film, and the chamber was under vacuum to minimize air scattering. Diffraction images were recorded on a Pilatus 1 M detector (Dectris Inc.) with an exposure time of 10 min and processed using the Nika software package in combination with WAXSTools in Igor Pro.

Synthesis. All monomers were previously synthesized.[57,58]

*General Procedure for the Synthesis of Polymers Using **P2** as the Example.* An oven-dried microwave vial containing a stir bar was charged in the glovebox with 3,6-dibromo-9 (2-ethylhexyl)-phenothiazine (0.350 g, 1.0 equiv), 3,6-dimethyl-*p*-phenylenediamine (1.05 equiv), $Pd(TFA)_2$ (0.05 equiv), Xphos (0.075 equiv), and NaO*t*Bu (2.8 equiv) and capped. The microwave vial was removed from the glovebox and freshly distilled, dried dioxane was added (5 mL), and the mixture was flushed with nitrogen. The reaction was heated in an oil bath at 100 °C for 24 h while being stirred vigorously. The reaction was allowed to cool to room temperature, and then chloroform was added to dilute the reaction mixture. The crude polymer was filtered through Celite, and the filtrate was concentrated under reduced pressure to give the crude polymer as a solid. Soxhlet extraction was performed with methanol, acetone, and hexanes to wash the impurities. Finally, the pure polymer (**P2**) was extracted as a blue solution in dichloromethane with 82% yield. The polymer was reprecipitated from methanol before the analysis.

RESULTS AND DISCUSSION

We began our study with the synthesis of nine polymers, **P1**−**P9** (Figure 1). In the first series, we maintain a small, branched alkyl group (2-ethylhexyl) on the phenothiazine nitrogen atom while changing the number of methyl groups on the PPDA core. Thus, **P1** has no methyl group, **P2** has two, and **P3** has four. Series 2 differs from series 1 with a larger alkyl group (2-hexyldecyl) on the phenothiazine core, and once again, **P4**, **P5**, and **P6** have zero, two, and four methyl groups on the PPDA core, respectively. Finally, series 3 has a *t*-butylphenyl group on the phenothiazine core, and **P7**, **P8**, and **P9** have zero, two, and four methyl groups, respectively, on the PPDA core.

The polymers were synthesized by the Buchwald/Hartwig reaction of 3,7-dibromophenothiazine containing the desired alkyl or aryl groups on the nitrogen with the corresponding PPDA containing zero, two, or four methyl groups according to our published report.[43] The solubility of the undoped polymers in a variety of solvents such as chloroform $CHCl_3$, tetrahydrofuran (THF), dichloromethane (DCM), *N*-methyl-2-pyrrolidone (NMP), and chlorobenzene (CB) increases as the number of methyl groups on PPDA increases. On the other hand, the doped polymers were soluble in more polar solvents such as dimethyl sulfoxide (DMSO), dimethylformamide (DMF), ethanol (EtOH), NMP, isopropanol (IPA), ethylene glycol, and *m*-cresol. The structures of the polymers were determined by ^{1}H NMR and FTIR. The ^{1}H NMR spectra for all of the polymers (Figure S1) have four regions; the aromatic region is around 6.5−7.2 ppm for all of the polymers except for **P3**, **P6**, and **P9** where the region shifts upfield due to the absence of the PPDA protons. The amine protons resonate around 5.0 and 5.2 ppm, whereas the protons of the alkyl group α to the nitrogen on the phenothiazine core show up around 3.5 ppm, except for **P7**−**P9**, where the substituent is the *t*-butylphenyl group. The alkyl region around 2.0 represents the protons of the methyl groups on the PPDA and between 1.0 and 1.5 for the other alkyl groups. The FTIR spectra were also consistent with the desired polymer products (Figure S2). Specifically, the alkyl C−H stretches are clearly visible for **P1**−**P6** containing the branched alkyl groups but not so much for **P7**−**P9**, which contain the *t*-butylphenyl group. While the aromatic C−H stretch (~3030 cm^{-1}) is not clearly visible for all of the polymers, the aromatic C═C stretch around 1500 cm^{-1} is clearly visible for all of the polymers.

https://doi.org/10.1021/acs.chemmater.3c02268
Chem. Mater. 2024, 36, 2279−2288

Following the structural determination of the polymers, they were subjected to size exclusion chromatography to determine their molecular weights. All of the polymers have similar number-average molecular weights (M_n) between 7 and 10 kDa against polystyrene standards with THF as the eluent (Table 1). The polydispersities were all below 2, and the degree of polymerization (DP) ranged from 16 to 24. Consequently, we reason that the molecular weight of the polymers would not be a major factor in any differences in their properties.

Table 1. Molecular Weight Determination of the Polymers

polymer	M_n (Da)	M_w (Da)	PDI	DP
P1	7000	10 500	1.50	16
P2	9100	11 900	1.23	19
P3	9700	15 100	1.56	19
P4	10 200	14 400	1.41	19
P5	9800	16 500	1.68	18
P6	8500	10 000	1.19	15
P7	10 200	18 700	1.83	24
P8	7800	15 500	1.99	17
P9	8600	12 500	1.44	18

To determine the best conditions for our study, we first checked the optimized conditions for processing the polymers. Consequently, we evaluated the effects of the solvent and dopant on the conductivity. The conductivity of the polymers was studied by using the four-point probe technique. **P2** was chosen as the standard for the experiment since we had previously reported its synthesis and application in a PSC.[43] We began by adopting our previously reported conditions with ethanol/*m*-cresol and 30% CSA as the solvent system and dopant, respectively. Furthermore, CSA has been previously studied as a dopant for PANI.[59−61] Ethanol/*m*-cresol gave low conductivity with 30% CSA, while DMSO as a cosolvent gave the highest conductivity, which was an order of magnitude higher than the others (Table S1). Therefore, the ethanol/DMSO solvent system was used to determine the effect of the amount of CSA dopant (based on mass) on the conductivity. As expected, the conductivity of the polymer increased as the percent of CSA increased. Surprisingly, a large percent of the dopant (50%) was required to obtain the highest conductivity (0.112 S/cm). Then, we investigated the effect of the type of dopants on the conductivity using the ethanol/DMSO solvent system and 50% dopant. Common dopants such as camphorsulfonic acid (CSA), dodecylbenzenesulfonic acid (DBSA), *p*-toluenesulfonic acid (PTSA), polystyrenesulfonic acid (PSS), and hydrochloric acid (HCl) were explored. The small molecule dopants gave better results than PSS. However, the conductivity of **P2** with 50% CSA as the dopant was higher than those of the others. Following these studies, we reinvestigate the cosolvents to determine their effect on the conductivity using 50% CSA as the dopant. It can be seen from Table 2 that films prepared from ethanol with DMSO as the cosolvent still recorded the highest conductivity (0.112 S/cm) relative to films prepared from ethanol or with other cosolvents. Based on these results, all of the polymers were processed from ethanol with DMSO as the cosolvent and 50% CSA as the dopant.

The absorption spectra of the polymers were analyzed in dichloromethane (DCM). The polymers are all blue in DCM, similar to our previous PANI derivatives, except for those containing the tetramethyl-substituted PPDA (**P3**, **P6**, and **P9**) (Figure 1b). We hypothesized that the difference in color for **P3**, **P6**, and **P9** is a result of severe twisting of the bonds between the phenothiazine core and the tetramethyl-substituted PPDA unit, resulting in a decrease in the conjugation length of the polymers. Evidence of this twisting can be seen in the UV data. The absorption spectrum was obtained for the polymers in their undoped and doped states (Figure 2). The undoped polymers all possess a maximum absorption wavelength (abs λ_{max}) between 530 and 630 nm (Figure 2a). The abs λ_{max} decreases as the number of methyl groups increase, which indicates twisting in the polymers' backbone due to torsional strain between the phenothiazine core and the PPDA unit as you go across the series (Table 3). Additionally, as you go between the series, the abs λ_{max} increased from series 1 to series 2 and then decreased for series 3. These changes are smaller (∼10 nm) compared to the changes across the series (∼30−40 nm), suggesting that the side chains on the phenothiazine core are not significantly different in solution (Table 3). As expected for PANI and its derivatives, there is a large red-shift in their absorption spectrum after doping to the emeraldine salt, as polaronic species are formed (Figure 2b). Formation of a polaronic band reduces the optical band gap. Additionally, the polymer chains tend to extend, which increases their conjugation length, further increasing the wavelength. Interestingly, **P3**, **P6**, and **P9** with the tetramethyl PPDA core in their structures possess shorter abs λ_{max} values than the other polymers. While polaronic bands formed in these polymers, the torsional strain in their backbones limits the extension in their effective conjugation length.

The thermal properties of the polymers are very important for their applications. TGA and DSC measurements were obtained to determine the thermal degradation (T_d) and glass transition (T_g) temperatures, respectively, of the polymers. All of the polymers have onset of thermal degradation (T_d onset)

Table 2. Optimization of the Conductivity with Solvents and Dopants

dopant effect		% dopant effect		solvent effect	
% dopant by mass	conductivity (S/cm)	dopant	conductivity (S/cm)	cosolvent	conductivity (S/cm)
10	0.007	CSA	0.112	EtOH	0.031
25	0.067	DBSA	0.022	DMSO	0.112
50	0.112	PTSA	0.063	DMF	0.083
>50	0.112	PSS	0.009	IPA	0.042
		HCl	0.072	*m*-cresol	0.003
				NMP	0.009
				ethylene glycol	0.044
				ethyl acetate	0.0004

https://doi.org/10.1021/acs.chemmater.3c02268
Chem. Mater. 2024, 36, 2279−2288

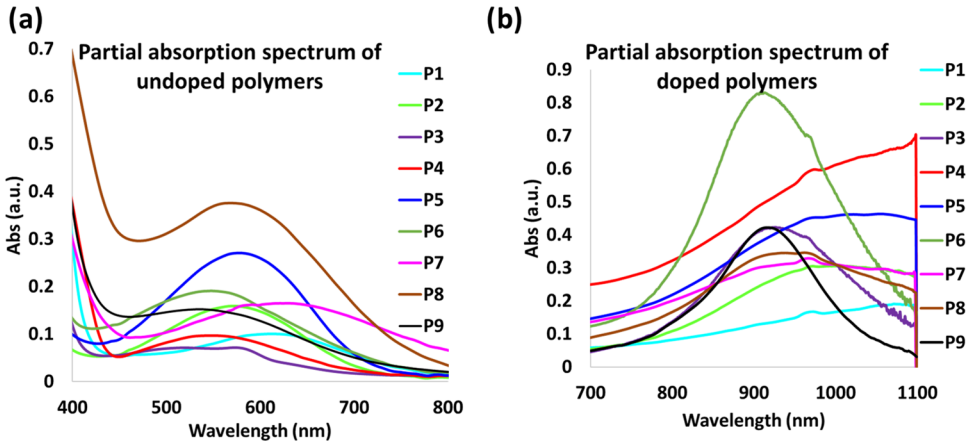

Figure 2. Partial absorption spectra of undoped polymers (a) and doped polymers (b).

Table 3. Absorption Maximum Wavelength of Doped and Undoped Polymers, Glass Transition Temperature, and Conductivity for P1−P9

polymers	abs λ_{max} undoped (nm)	abs λ_{max} doped (nm)	T_g (°C)	conductivity (S/cm)
P1	612	1072	107	$3.42 \times 10^{-1} \pm 4.40 \times 10^{-1}$
P2	572	1076	119	$1.42 \times 10^{-1} \pm 1.70 \times 10^{-1}$
P3	520	926	130	$5.72 \times 10^{-2} \pm 4.80 \times 10^{-2}$
P4	627	1098	82	$1.05 \times 10^{-1} \pm 9.07 \times 10^{-3}$
P5	578	1056	92	$6.70 \times 10^{-2} \pm 1.48 \times 10^{-3}$
P6	548	920	104	$2.12 \times 10^{-2} \pm 1.99 \times 10^{-3}$
P7	630	1096	160	$2.53 \times 10^{-1} \pm 2.72 \times 10^{-3}$
P8	568	938	175	$1.51 \times 10^{-1} \pm 4.40 \times 10^{-3}$
P9	535	917	190	$2.17 \times 10^{-2} \pm 3.51 \times 10^{-4}$

above 300 °C, and they do not completely degrade under a nitrogen atmosphere (Figure S3), demonstrating their high thermal stability. Moreover, the polymers show interesting behavior when subjected to DSC. We were unable to identify any thermal transitions for the polymers in the doped state due to the presence of the CSA dopant having a very large melting transition that suppresses the polymers' thermal transitions. Therefore, the polymers were processed as powder in the undoped state before being subjected to DSC (Figure S4). The polymers were reprecipitated from methanol several times and dried in a vacuum oven at 60 °C overnight before the experiment was performed. In all of the series, the T_g of the polymers increased as the number of methyl groups on the PPDA increased. These results indicate that the increased bulk in the polymers' backbones increased their rigidity (due to torsional strain), thus decreasing the free volume in the polymers' backbone (Table 3). On the other hand, series 2 possesses the lowest overall T_g among the series, followed by series 1, meaning that the larger, branched alkyl groups, while they may be good for solubility, are poor for packing (interchain interactions) of the polymer chains. This notion can be seen in the optimized structures of the phenothiazine core containing the side chains (Figure S5). The branched alkyl chains on **P1−P6** lie close to the phenothiazine core, which is already nonplanar. The presence of the large alkyl chains hinders extensive interactions between polymer chains; thus, the polymer chains have more freedom to slide past each other, which lowers the T_g. On the other hand, the *t*-butylphenyl substituent provides a more rigid structure, which results in a more planar phenothiazine core. Thus, the polymers with the *t*-butylphenyl substituent had the highest T_g, due to the rigidity in the polymer's backbone compared to the branch alkyl groups. Based on these results, we hypothesized that the polymers containing the *t*-butylphenyl side chains would result in better packing of the polymer chains after doping, leading to higher conductivity.

The conductivity of the polymers was determined using 50% CSA as the dopant and EtOH/DMSO as the solvent and cosolvent. Here, the films were prepared from a precise concentration, and a specified amount of the polymers was drop-casted from solution and dried slowly over a small vapor of DMSO. All of the polymers had good conductivity on the order of 10^{-1}−10^{-2} S/cm. As expected, the polymers with 0 and 2 methyl groups have a higher conductivity than the polymers with four methyl groups in all three series (Table 3). On average, series 1 and series 3 outperformed series 2 (Figure 3). The low performance of series 2 could be a result of the

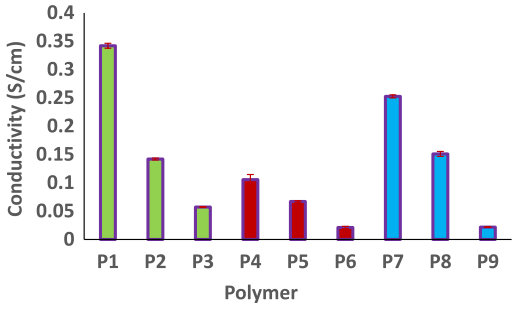

Figure 3. Comparison of the conductivity for **P1−P9**. Series 1 (green), series 2 (red), and series 3 (blue).

bulkier 2-hexyldecyl side chain, which decreases the interactions between the polymer chains and reduces charge transfer between chains. Interestingly, series 1 has a conductivity slightly higher than that of series 3, despite the small curvature of the phenothiazine core of series 1, which is expected to affect the packing. Nevertheless, the bulky tetramethyl PPDA unit contributed most to the decrease in the conductivity because of the torsional strain in the polymer chains. Since the T_g data indicate that the polymers are mostly disordered, we propose that the dominant factor in the conductivity is based on a multiscale charge transport phenomena where the movement of charge occurs in a

https://doi.org/10.1021/acs.chemmater.3c02268
Chem. Mater. 2024, 36, 2279−2288

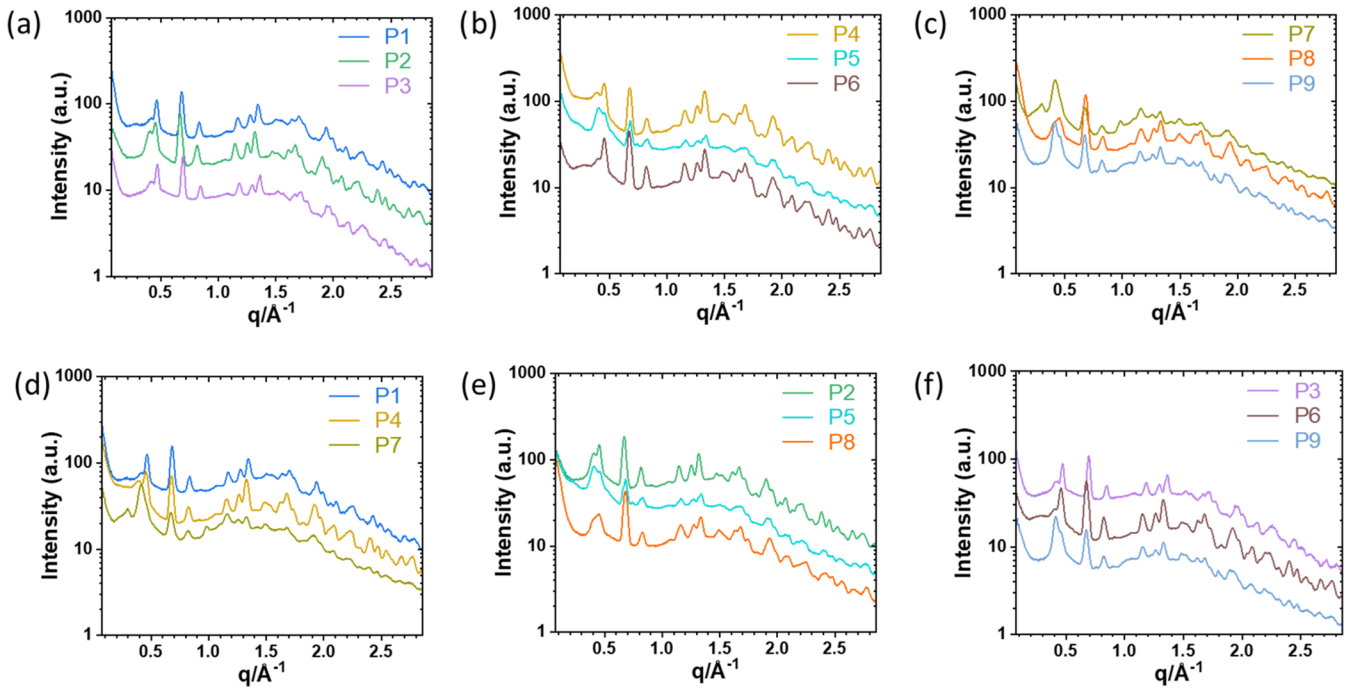

Figure 4. WAXS spectra for **P1**−**P9** doped with 50% CSA. Comparison of **P1**−**P9** based on series (a−c) and based on substituents on phenothiazine side chains (d−f).

disordered lattice on different scales (short scale gives high mobility and large scale gives low mobility).[47,62] This hypothesis is supported by the trend within each series where the conductivity decreased as the torsional strain, and thus disorder, increased in the polymer chains.[63]

The polymers were then subjected to wide-angle X-ray scattering (WAXS) to ascertain their molecular packing, which is linked to their conductivity performance. The polymers were first prepared as films and then crushed to obtain a powder. We first explored **P2** as our control and investigated its diffraction pattern with different amounts of CSA dopant (0, 10, 25, 50%). In Figure S6, the undoped polymer (0% CSA) showed two peaks at q = 0.75 and 2.37 A^{-1}, which signifies the presence of some short-range ordered crystallites and aromatic interactions, which is probably difficult to observe in the DSC.[64] On the other hand, CSA is highly crystalline with several peaks in the region of q = 0.5−2.0 A^{-1}. Upon doping of **P2** with 10 and 25% CSA, the peaks at q = 0.75 and 2.37 A^{-1} disappeared. However, when the polymer was doped with 50% CSA, several well-defined scattering peaks in the wide-angle scattering region were observed in the diffraction pattern, indicating the presence of phase-separated CSA that forms an individual crystalline domain. Noteworthy, two peaks occurred in the region of q = 0.45 and 0.67 A^{-1}, which is attributed to the interaction of the side chains with the dopant. Consequently, we evaluated all of the polymer at 50% dopant to determine if a similar pattern would be observed (Figure 4). The polymers are compared based on their series (Figure 4a−4c) as well as the substituents on the phenothiazine core (Figure 4d−4f). All of the polymers showed obvious phase separation in the crystalline domain of CSA in the region of q = 0.5−2 A^{-1}; therefore, we are not able to determine any aromatic interactions in the backbone. Thus, we focused our comparison on the alkyl chain stacking region for all the polymers. **P1**−**P6** showed strong scattering peaks of the alkyl chain (Figure 4a,b) at q = 0.45−0.47 A^{-1}, while **P7**−**P9** had weaker scattering in this region (Figure 4c). Additionally, all of the polymers have a strong peak at q = 0.67−0.69 A^{-1}, where the side chains are presumed to interact with the dopant. These results suggest that there are similar interactions of the dopant with the side chains; however, **P7**−**P9** may have different side chain packing compared to **P1**−**P6** (Figure 4d,f). Unfortunately, we were not able to observe any of the possible interactions within the polymers' backbone; however, based on the broadness in the region between q = 1.0 and 2.0 A^{-1}, we can speculate that the polymers' backbones are mostly amorphous. Consequently, we extend the study to look at the surface of the polymers' films with SEM and AFM to determine if there are any abnormalities in the films.

We analyzed the morphology of the polymers in their doped state with SEM imaging. We first investigated the films under different processing conditions. Since we have been using **P2** as our standard, we explored its films with various percentages of dopant (0, 10, 25, and 50%) (Figure S7), as the dopants can cause extreme morphological changes due to the swelling and plasticizing effects.[65] From these images, it can be seen that the films become smoother as the amount of dopant increased from 0 to 50%. These data corroborate what we see in the conductivity measurements where the highest conductivity is obtained from 50% doped polymers (Table 2). We then analyzed the surface morphology of all of the films with 50% dopant by using SEM (Figure S8). While all of the films were very smooth, we observed cracking in them, which we speculate arose from the extended vacuum process required for SEM imaging. During this process, the moisture is removed from the films, which then peel from the surface of the substrate, leading to cracking. To check the morphology of the films under conditions closest to the operation conditions, we performed AFM imaging to analyze the surface of the films for cracking or any abnormal features. Once again, as the amount of dopant increased from 0 to 50%, the surface of the films became more uniform and smoother (Figure 5a). Figure 5b

https://doi.org/10.1021/acs.chemmater.3c02268
Chem. Mater. 2024, 36, 2279−2288

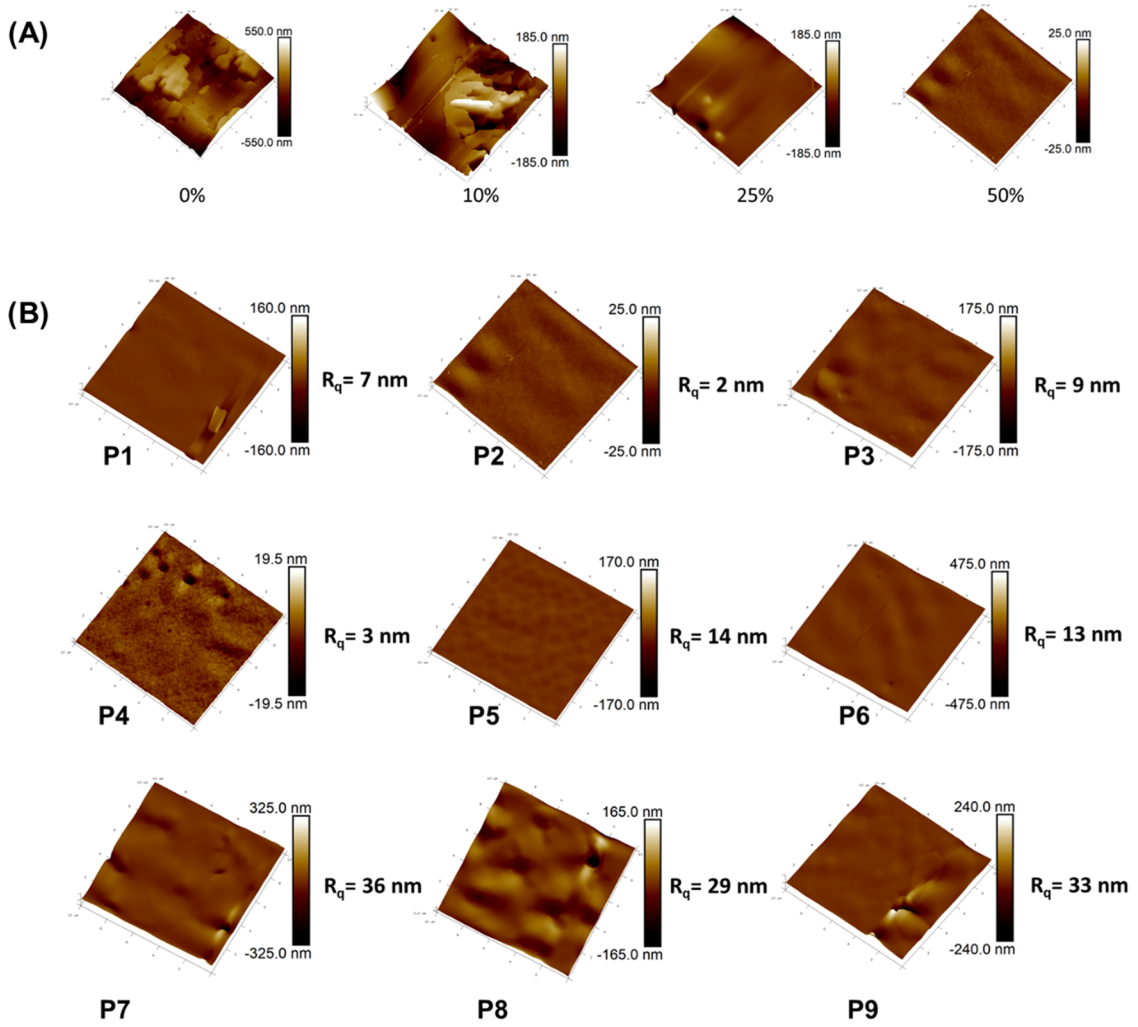

Figure 5. AFM images showing the effect of percent dopant of **P2** (A) and dopant on the films' surface morphology of **P1**−**P9** (B).

shows the AFM images for all of the polymers (**P1**−**P9**) with 50% dopant. All the films' surfaces were uniform in coverage and without cracking. From all our data, it is clear that the polymers mostly behave in a similar manner with only small changes in the side chains on the phenothiazine core and the PPDA unit that dominated the conductivity.

CONCLUSIONS

Side chains are important for conjugated polymer as they enhance the polymer's solubility. However, they also influence the packing of the polymer chains, which impacts their performances. Subsequently, understanding their effects on the polymer chain arrangements is of upmost importance. In this study, we prepared nine PANI derivatives from the phenothiazine core and PPDA unit. These polymers contained branched alkyl groups and *t*-butylphenyl as the substituents on the phenothiazine core and different amounts of methyl group on the PPDA. We discovered that both the side chains on the phenothiazine core and the methyl groups on the PPDA unit created disorder within the polymer. Noteworthy, the 2-hexyldecyl group, while it makes good quality films, seems to disrupt packing more than the other side chains, which lowers their performances. Additionally, the *t*-butylphenyl group is also a great substituent that aids in the solubility of the polymer and displays conductivity on par with the commonly used 2-ethylhexyl group. However, the most substantial hindrance to conductivity of the polymers is the presence of the tetramethyl groups on the PPDA unit, perhaps due to twisting in the polymers' backbones. To our knowledge, this is the first example of a dual comparison of N-substituted and aryl-substituted side chains on PANI derivatives on conductivity. In addition, we provide direct comparison of the commonly used branched alkyl group side chains to the *t*-butylphenyl side group in conducting polymers on their performances. Our findings emphasize the significance of side chains in modulating conductivity and morphology in PANI derivatives. These findings will help tune the dimensions of solubilizing side chains to facilitate the effective processing of conjugated polymers while mitigating the adverse effects at the device level that sometimes result from the choice a location of the side chains.

ASSOCIATED CONTENT

Supporting Information

The Supporting Information is available free of charge at https://pubs.acs.org/doi/10.1021/acs.chemmater.3c02268.

^{1}H NMR, FTIR, DSC, TGA, SEM, and GIWAXS (PDF)

https://doi.org/10.1021/acs.chemmater.3c02268
Chem. Mater. 2024, 36, 2279−2288

AUTHOR INFORMATION

Corresponding Author

Colleen N. Scott − *Department of Chemistry, Mississippi State University, Mississippi State, Mississippi 39762, United States;* orcid.org/0000-0003-3332-2439; Email: cscott@chemistry.msstate.edu

Authors

Hari Giri − *Department of Chemistry, Mississippi State University, Mississippi State, Mississippi 39762, United States*

Guorong Ma − *School of Polymer Science and Engineering, Center for Optoelectronic Materials and Devices, The University of Southern Mississippi, Hattiesburg, Mississippi 39406, United States*

Mohammed Almtiri − *Department of Chemistry, Mississippi State University, Mississippi State, Mississippi 39762, United States;* orcid.org/0000-0002-4108-0604

Xiaodan Gu − *School of Polymer Science and Engineering, Center for Optoelectronic Materials and Devices, The University of Southern Mississippi, Hattiesburg, Mississippi 39406, United States;* orcid.org/0000-0002-1123-3673

Complete contact information is available at: https://pubs.acs.org/10.1021/acs.chemmater.3c02268

Author Contributions

The manuscript was written through the contributions of all authors. All authors have given their approval to the final version of the manuscript.

Funding

The authors are grateful for the financial support from the National Science Foundation for an award (CHE-1945503) and the Office of Nava Research for award N00014-23-1-2063.

Notes

The authors declare no competing financial interest.

REFERENCES

(1) Shirakawa, H.; Louis, E. J.; MacDiarmid, A. G.; Chiang, C. K.; Heeger, A. J. Synthesis of electrically conducting organic polymers: halogen derivatives of polyacetylene, (CH)x. *J. Chem. Soc., Chem. Commun.* **1977**, No. 16, 578−580.

(2) Vidal, J.-C.; Garcia-Ruiz, E.; Castillo, J.-R. Recent Advances in Electropolymerized Conducting Polymers in Amperometric Biosensors. *Microchim. Acta* **2003**, *143* (2), 93−111.

(3) Unsworth, J.; Lunn, B. A.; Innis, P. C.; Jin, Z.; Kaynak, A.; Booth, N. G. Technical Review: Conducting Polymer Electronics. *J. Intell. Mater. Syst. Struct.* **1992**, *3* (3), 380−395, DOI: 10.1177/1045389X9200300301.

(4) Schoch, K. F. Update on electrically conductive polymers and their applications. *IEEE Electr. Insul. Mag.* **1994**, *10* (3), 29−32, DOI: 10.1109/57.285420.

(5) Angelopoulos, M. Conducting polymers in microelectronics. *IBM J. Res. Dev.* **2001**, *45* (1), 57−75.

(6) Das, T. K.; Prusty, S. Review on Conducting Polymers and Their Applications. *Polym.-Plast. Technol. Eng.* **2012**, *51* (14), 1487−1500, DOI: 10.1080/03602559.2012.710697.

(7) Cao, Y.; Smith, P.; Heeger, A. J. Counter-ion induced processibility of conducting polyaniline and of conducting polyblends of polyaniline in bulk polymers. *Synth. Met.* **1992**, *48* (1), 91−97.

(8) MacDiarmid, A. G.; Epstein, A. J. Polyanilines: a novel class of conducting polymers. *Faraday Discuss. Chem. Soc.* **1989**, *88* (0), 317−332, DOI: 10.1039/dc9898800317.

(9) Jangid, N. K.; Chauhan, N. S.; Meghwal, K.; Ameta, R.; Punjabi, P. B. A review: conducting polymers and their applications. *Res. J. Pharm., Biol. Chem. Sci.* **2014**, *5* (3), 383−412.

(10) Chen, F.; Liu, P. Conducting Polyaniline Nanoparticles and Their Dispersion for Waterborne Corrosion Protection Coatings. *ACS Appl. Mater. Interfaces* **2011**, *3* (7), 2694−2702.

(11) Deshpande, P. P.; Jadhav, N. G.; Gelling, V. J.; Sazou, D. Conducting polymers for corrosion protection: a review. *J. Coat. Technol. Res.* **2014**, *11* (4), 473−494.

(12) Huang, W. S.; Angelopoulos, M.; White, J. R.; Park, J. M. Metallization of Printed Circuit Boards Using Conducting Polyaniline. *Mol. Cryst. Liq. Cryst.* **1990**, *189* (1), 227−235, DOI: 10.1080/00268949008037235.

(13) Soto-Oviedo, M. A.; Araújo, O. A.; Faez, R.; Rezende, M. C.; De Paoli, M.-A. Antistatic coating and electromagnetic shielding properties of a hybrid material based on polyaniline/organoclay nanocomposite and EPDM rubber. *Synth. Met.* **2006**, *156* (18), 1249−1255.

(14) Kobayashi, T.; Yoneyama, H.; Tamura, H. Polyaniline film-coated electrodes as electrochromic display devices. *J. Electroanal. Chem. Interfacial Electrochem.* **1984**, *161* (2), 419−423.

(15) Dhawale, D. S.; Vinu, A.; Lokhande, C. D. Stable nanostructured polyaniline electrode for supercapacitor application. *Electrochim. Acta* **2011**, *56* (25), 9482−9487.

(16) Eftekhari, A.; Li, L.; Yang, Y. Polyaniline supercapacitors. *J. Power Sources* **2017**, *347*, 86−107.

(17) Mei, Y.; Shen, Z.; Kundu, S.; Dennis, E.; Pang, S.; Tan, F.; Yue, G.; Gao, Y.; Dong, C.; Liu, R.; Zhang, W.; Saidaminov, M. I. Perovskite Solar Cells with Polyaniline Hole Transport Layers Surpassing a 20% Power Conversion Efficiency. *Chem. Mater.* **2021**, *33* (12), 4679−4687.

(18) Lee, K.; Yu, H.; Lee, J. W.; Oh, J.; Bae, S.; Kim, S. K.; Jang, J. Efficient and moisture-resistant hole transport layer for inverted perovskite solar cells using solution-processed polyaniline. *J. Mater. Chem. C* **2018**, *6* (23), 6250−6256, DOI: 10.1039/C8TC01870G.

(19) Al-Dainy, G. A.; Watanabe, F.; Kannarpady, G. K.; Ghosh, A.; Berry, B.; Biris, A. S.; Bourdo, S. E. Optimizing Lignosulfonic Acid-Grafted Polyaniline as a Hole-Transport Layer for Inverted CH3NH3PbI3 Perovskite Solar Cells. *ACS Omega* **2020**, *5* (4), 1887−1901.

(20) Fehse, K.; Schwartz, G.; Walzer, K.; Leo, K. Combination of a polyaniline anode and doped charge transport layers for high-efficiency organic light emitting diodes. *J. Appl. Phys.* **2007**, *101* (12), No. 124509.

(21) Zhang, R.; Ma, H.; Wang, B. Removal of Chromium(VI) from Aqueous Solutions Using Polyaniline Doped with Sulfuric Acid. *Ind. Eng. Chem. Res.* **2010**, *49* (20), 9998−10004.

(22) Nasar, A.; Mashkoor, F. Application of polyaniline-based adsorbents for dye removal from water and wastewater-a review. *Environ. Sci. Pollut Res.* **2019**, *26* (6), 5333−5356.

(23) Dhand, C.; Das, M.; Datta, M.; Malhotra, B. D. Recent advances in polyaniline based biosensors. *Biosens. Bioelectron.* **2011**, *26* (6), 2811−2821.

(24) Zarrintaj, P.; Vahabi, H.; Saeb, M. R.; Mozafari, M. Chapter 14 - Application of Polyaniline and Its Derivatives. In *Fundamentals and Emerging Applications of Polyaniline*; Mozafari, M.; Chauhan, N. P. S., Eds.; Elsevier, 2019; pp 259−272.

(25) Marques, A. S.; Szostak, R.; Marchezi, P. E.; Nogueira, A. F. Perovskite solar cells based on polyaniline derivatives as hole transport materials. *J. Phys.: Energy* **2019**, *1* (1), No. 015004.

(26) Athawale, A. A.; Kulkarni, M. V. Polyaniline and its substituted derivatives as sensor for aliphatic alcohols. *Sens. Actuators, B* **2000**, *67* (1), 173−177.

(27) Mustafin, A. G.; Latypova, L. R.; Andriianova, A. N.; Mullagaliev, I. N.; Salikhov, S. M.; Salikhov, R. B.; Usmanova, G. S. Polymerization of new aniline derivatives: synthesis, characterization and application as sensors. *RSC Adv.* **2021**, *11* (34), 21006−21016.

(28) Ahmad, S.; Ashraf, S. M.; Riaz, U.; Zafar, S. Development of novel waterborne poly(1-naphthylamine)/poly(vinylalcohol)−resorcinol formaldehyde-cured corrosion resistant composite coatings. *Prog. Org. Coat.* **2008**, *62* (1), 32−39.

(29) Riaz, U.; Khan, S.; Islam, M. N.; Ahmad, S.; Ashraf, S. M. Evaluation of antibacterial activity of nanostructured poly(1-naphthylamine) and its composites. *J. Biomater. Sci., Polym. Ed.* **2008**, *19* (11), 1535−1546, DOI: 10.1163/156856208786140418.
(30) Riaz, U.; Ahmad, S. A.; Ashraf, S. M.; Ahmad, S. Effect of dopant on the corrosion protective performance of environmentally benign nanostructured conducting composite coatings. *Prog. Org. Coat.* **2009**, *65* (3), 405−409.
(31) Riaz, U.; Ashraf, S. M.; Budhiraja, V.; Aleem, S.; Kashyap, J. Comparative studies of the photocatalytic and microwave − assisted degradation of alizarin red using ZnO/poly(1- naphthylamine) nanohybrids. *J. Mol. Liq.* **2016**, *216*, 259−267.
(32) Riaz, U.; Ashraf, S. M. Synergistic effect of microwave irradiation and conjugated polymeric catalyst in the facile degradation of dyes. *RSC Adv.* **2014**, *4* (88), 47153−47162.
(33) Tran, M. T.; Nguyen, T. H. T.; Vu, Q. T.; Nguyen, M. V. Properties of poly(1-naphthylamine)/Fe3O4 composites and arsenic adsorption capacity in wastewater. *Front. Mater. Sci.* **2016**, *10* (1), 56−65.
(34) Ma, L.; Huang, C.-Q.; Gan, M.-Y. Synthesis and anticorrosion properties of poly(2,3-dimethylaniline) doped with phosphoric acid. *J. Appl. Polym. Sci.* **2013**, *127* (5), 3699−3704.
(35) Ma, L.; Wei, S.-j.; Gan, M.-y.; Chen, F.-f.; Tian, N.; Zeng, J. Rapid emuision polymerization of poly (2, 3-dimethylaniline) initiated by APS/Fe2+ composite oxidants and its performances. *Acta Polym. Sin.* **2013**, No. 8, 1033−1038.
(36) Sathiyanarayanan, S.; Dhawan, S. K.; Trivedi, D. C.; Balakrishnan, K. Soluble conducting poly ethoxy aniline as an inhibitor for iron in HCl. *Corros. Sci.* **1992**, *33* (12), 1831−1841.
(37) Savitha, P.; Sathyanarayana, D. N. Synthesis and characterization of soluble conducting poly(o-/m-toluidine-co-o-nitroaniline). *Synth. Met.* **2004**, *145* (2), 113−118.
(38) Hwang, G.-W.; Wu, K.-Y.; Hua, M.-Y.; Lee, H.-T.; Chen, S.-A. Structures and properties of the soluble polyanilines, N-alkylated emeraldine bases. *Synth. Met.* **1998**, *92* (1), 39−46.
(39) Kong, X.; Kulkarni, A. P.; Jenekhe, S. A. Phenothiazine-Based Conjugated Polymers: Synthesis, Electrochemistry, and Light-Emitting Properties. *Macromolecules* **2003**, *36* (24), 8992−8999.
(40) Ponder, J. F., Jr.; Gregory, S. A.; Atassi, A.; Menon, A. K.; Lang, A. W.; Savagian, L. R.; Reynolds, J. R.; Yee, S. K. Significant Enhancement of the Electrical Conductivity of Conjugated Polymers by Post-Processing Side Chain Removal. *J. Am. Chem. Soc.* **2022**, *144* (3), 1351−1360.
(41) Almtiri, M.; Dowell, T. J.; Chu, I.; Wipf, D. O.; Scott, C. N. Phenoxazine-Containing Polyaniline Derivatives with Improved Electrochemical Stability and Processability. *ACS Appl. Polym. Mater.* **2021**, *3* (6), 2988−2997.
(42) Almtiri, M.; Dowell, T. J.; Giri, H.; Wipf, D. O.; Scott, C. N. Electrochemically Stable Carbazole-Derived Polyaniline for Pseudocapacitors. *ACS Appl. Polym. Mater.* **2022**, *4* (5), 3088−3097.
(43) Qi, Y.; Almtiri, M.; Giri, H.; Jha, S.; Ma, G.; Shaik, A. K.; Zhang, Q.; Pradhan, N.; Gu, X.; Hammer, N. I.; Patton, D.; Scott, C.; Dai, Q. Evaluation of the Passivation Effects of PEDOT:PSS on Inverted Perovskite Solar Cells. *Adv. Energy Mater.* **2022**, *12* (46), No. 2202713, DOI: 10.1002/aenm.202202713.
(44) Liu, Y.; Niu, Z.; Dai, G.; Chen, Y.; Li, H.; Huang, L.; Zhang, X.; Xu, Y.; Zhao, Y. Phenothiazine-based copolymer with redox functional backbones for organic battery cathode materials. *Mater. Today Energy* **2021**, *21*, No. 100812.
(45) Mei, J.; Bao, Z. Side Chain Engineering in Solution-Processable Conjugated Polymers. *Chem. Mater.* **2014**, *26* (1), 604−615.
(46) Das, M. K.; Hameed, F.; Lillis, R.; Gavvalapalli, N. A twist in the non-slanted H-mers to control π-conjugation in 2-dimensions and optical properties. *Mater. Adv.* **2020**, *1* (8), 2917−2925.
(47) Park, K. S.; Kwok, J. J.; Kafle, P.; Diao, Y. When Assembly Meets Processing: Tuning Multiscale Morphology of Printed Conjugated Polymers for Controlled Charge Transport. *Chem. Mater.* **2021**, *33* (2), 469−498.
(48) Dong, B. X.; Nowak, C.; Onorato, J. W.; Strzalka, J.; Escobedo, F. A.; Luscombe, C. K.; Nealey, P. F.; Patel, S. N. Influence of Side-Chain Chemistry on Structure and Ionic Conduction Characteristics of Polythiophene Derivatives: A Computational and Experimental Study. *Chem. Mater.* **2019**, *31* (4), 1418−1429.
(49) Chen, X.; Zhang, Z.; Ding, Z.; Liu, J.; Wang, L. Diketopyrrolopyrrole-based Conjugated Polymers Bearing Branched Oligo(Ethylene Glycol) Side Chains for Photovoltaic Devices. *Angew. Chem., Int. Ed.* **2016**, *55* (35), 10376−10380.
(50) Carpenter, J. H.; Ghasemi, M.; Gann, E.; Angunawela, I.; Stuard, S. J.; Rech, J. J.; Ritchie, E.; O'Connor, B. T.; Atkin, J.; You, W.; DeLongchamp, D. M.; Ade, H. Competition between Exceptionally Long-Range Alkyl Sidechain Ordering and Backbone Ordering in Semiconducting Polymers and Its Impact on Electronic and Optoelectronic Properties. *Adv. Funct. Mater.* **2019**, *29* (5), No. 1806977.
(51) Liao, G.; Li, Q.; Xu, Z. The chemical modification of polyaniline with enhanced properties: A review. *Prog. Org. Coat.* **2019**, *126*, 35−43.
(52) Bhadra, S.; Khastgir, D.; Singha, N. K.; Lee, J. H. Progress in preparation, processing and applications of polyaniline. *Prog. Polym. Sci.* **2009**, *34* (8), 783−810.
(53) Zhang, Y.; Rutledge, G. C. Electrical Conductivity of Electrospun Polyaniline and Polyaniline-Blend Fibers and Mats. *Macromolecules* **2012**, *45* (10), 4238−4246.
(54) Bhadra, S.; Khastgir, D. Determination of crystal structure of polyaniline and substituted polyanilines through powder X-ray diffraction analysis. *Polym. Test.* **2008**, *27* (7), 851−857.
(55) Gadisa, A.; Oosterbaan, W. D.; Vandewal, K.; Bolsée, J.-C.; Bertho, S.; D'Haen, J.; Lutsen, L.; Vanderzande, D.; Manca, J. V. Effect of Alkyl Side-Chain Length on Photovoltaic Properties of Poly(3-alkylthiophene)/PCBM Bulk Heterojunctions. *Adv. Funct. Mater.* **2009**, *19* (20), 3300−3306.
(56) Zhang, Z.-G.; Min, J.; Zhang, S.; Zhang, J.; Zhang, M.; Li, Y. Alkyl chain engineering on a dithieno[3,2-b:2′,3′-d]silole-alt-dithienylthiazolo[5,4-d]thiazole copolymer toward high performance bulk heterojunction solar cells. *Chem. Commun.* **2011**, *47* (33), 9474−9476.
(57) Yun, D.-H.; Yoo, H.-S.; Seong, K.-H.; Lim, J.-H.; Park, Y.-S.; Woo, J.-W. Synthesis, Photovoltaic Properties and Side-chain Effect of Copolymer Containing Phenothiazine and 2,1,3-Benzothiadiazole. *Appl. Chem. Eng.* **2014**, *25* (5), 487−496, DOI: 10.14478/ace.2014.1068.
(58) Kim, S.-K.; Lee, C.-J.; Park, J.-W.; Oh, S.-Y. Synthesis and Hole-Injection Property of Phenothiazinyl Derivative Containing Triphenylamine Moiety in OLED Device. *Mol. Cryst. Liq. Cryst.* **2007**, *470* (1), 231−239, DOI: 10.1080/15421400701495690.
(59) Pouget, J. P.; Oblakowski, Z.; Nogami, Y.; Albouy, P. A.; Laridjani, M.; Oh, E. J.; Min, Y.; MacDiarmid, A. G.; Tsukamoto, J.; Ishiguro, T.; Epstein, A. J. Recent structural investigations of metallic polymers. *Synth. Met.* **1994**, *65* (2), 131−140.
(60) Pouget, J. P.; Hsu, C. H.; Mac Diarmid, A. G.; Epstein, A. J. Structural investigation of metallic PAN-CSA and some of its derivatives. *Synth. Met.* **1995**, *69* (1), 119−120.
(61) Cao, Y.; Smith, P.; Heeger, A. J. Counter-ion induced processibility of conducting polyaniline. *Synth. Met.* **1993**, *57* (1), 3514−3519.
(62) Noriega, R.; Salleo, A.; Spakowitz, A. J. Chain conformations dictate multiscale charge transport phenomena in disordered semiconducting polymers. *Proc. Natl. Acad. Sci. U.S.A.* **2013**, *110* (41), 16315−16320.
(63) Westenhoff, S.; Beenken, W. J.; Yartsev, A.; Greenham, N. C. Conformational disorder of conjugated polymers. *J. Chem. Phys.* **2006**, *125* (15), No. 154903, DOI: 10.1063/1.2358682.
(64) Peng, Z.; Ye, L.; Ade, H. Understanding, quantifying, and controlling the molecular ordering of semiconducting polymers: from novices to experts and amorphous to perfect crystals. *Mater. Horiz.* **2022**, *9* (2), 577−606.

(65) Wang, X.-S.; Tang, H.-P.; Li, X.-D.; Hua, X. Investigations on the Mechanical Properties of Conducting Polymer Coating-Substrate Structures and Their Influencing Factors. *Int. J. Mol. Sci.* **2009**, *10* (12), 5257−5284.

https://doi.org/10.1021/acs.chemmater.3c02268
Chem. Mater. 2024, 36, 2279−2288